MDPI

Article

Effect of Exportin 1/XPO1 Nuclear Export Pathway Inhibition on Coronavirus Replication

Masmudur M. Rahman [1,2,3,*], **Bereket Estifanos** [2,4], **Honor L. Glenn** [3,4], **Ami D. Gutierrez-Jensen** [1], **Karen Kibler** [5], **Yize Li** [3,5], **Bertram Jacobs** [3,5], **Grant McFadden** [3] and **Brenda G. Hogue** [2,3,4,*]

[1] Center for Personalized Diagnostics, Biodesign Institute, Arizona State University, Tempe, AZ 85287, USA; adave@asu.edu

[2] School of Life Sciences Microbiology Graduate Program, Arizona State University, Tempe, AZ 85287, USA; bestifan@asu.edu

[3] School of Life Sciences, Arizona State University, Tempe, AZ 85287, USA; honor.glenn@asu.edu (H.L.G.); yize.li.2@asu.edu (Y.L.); bjacobs@asu.edu (B.J.); grantmcf@asu.edu (G.M.)

[4] Center for Applied Structural Discovery, Biodesign Institute, Arizona State University, Tempe, AZ 85287, USA

[5] Center for ASU-Banner Neurodegenerative Disease Research, Biodesign Institute, Arizona State University, Tempe, AZ 85287, USA; karen.kibler@asu.edu

[*] Correspondence: masmudur.rahman@asu.edu (M.M.R.); brenda.hogue@asu.edu (B.G.H.)

Abstract: The nucleocytoplasmic transport of proteins using XPO1 (exportin 1) plays a vital role in cell proliferation and survival. Many viruses also exploit this pathway to promote infection and replication. Thus, inhibiting the XPO1-mediated nuclear export pathway with selective inhibitors has a diverse effect on virus replication by regulating antiviral, proviral, and anti-inflammatory pathways. The XPO1 inhibitor Selinexor is an FDA-approved anticancer drug predicted to have antiviral or proviral functions against viruses. Here, we observed that the pretreatment of cultured cell lines from human or mouse origin with the nuclear export inhibitor Selinexor significantly enhanced the protein expression and replication of mouse hepatitis virus (MHV), a mouse coronavirus. The knockdown of cellular XPO1 protein expression also significantly enhanced the replication of MHV in human cells. However, for SARS-CoV-2, Selinexor treatment had diverse effects on virus replication in different cell lines. These results indicate that XPO1-mediated nuclear export pathway inhibition might affect coronavirus replication depending on cell types and virus origin.

Keywords: XPO1; exportin 1; nuclear export inhibitor; coronavirus; mouse hepatitis virus; SARS-CoV-2; Selinexor; virus replication

1. Introduction

The nucleocytoplasmic transport of proteins and other molecules is a highly regulated cellular process. Many nuclear export (called exportins) and import (called importins) proteins are involved in this process by exploiting nuclear pore complexes that form proteinaceous channels in the nuclear envelope [1,2]. Exportin 1 (XPO1), also known as CRM1 (chromosome region maintenance 1), is one of the major nuclear export proteins, transporting hundreds of cellular cargo proteins involved in diverse cellular processes such as transcription, translation, cellular growth, differentiation, and mediating inflammatory responses that include antiviral pathways [3,4]. Thus, the direct inhibition of XPO1 function has been explored as a potential antiviral and anticancer therapeutic target [5–8]. Various natural or chemically synthesized small molecules that bind to XPO1 and block

the export of XPO1 cargo proteins from the nucleus to the cytoplasm have been developed [9,10]. Collectively, these molecules are known as selective inhibitors of nuclear export (SINEs). SINEs have been shown to have anticancer activity against diverse types of human cancers, and at least one modified drug version with an increased safety profile, called Selinexor, has been approved by the FDA for treating multiple myeloma and diffuse large B-cell lymphoma [11,12]. SINEs are also reported in the literature to have antiviral activity against RNA viruses like influenza and respiratory syncytial virus (RSV) that cause respiratory infections by blocking key cellular processes and virus-mediated hijacking of the nucleocytoplasmic transport process [6,13,14].

Coronaviruses are enveloped, positive-sense RNA viruses that are known to infect humans and animals. At least seven coronaviruses are known to infect humans. Coronaviruses 229E, NL63, OC43, and HKU1 infect people around the world to cause the common cold [15]. Other coronaviruses, MERS-CoV, SARS-CoV, and SARS-CoV-2, are responsible for major disease outbreaks and cause high mortality [16]. In nature, bats are known to be primary reservoirs of many coronaviruses, from where viruses spill over to intermediate animals such as palm civet, pangolins, rodents, camels, pigs, and cattle, where these viruses evolve and then spillover to humans, causing mild to severe disease [17,18]. The rapid emergence of different variants of SARS-CoV-2 indicates that the viral genome acquires multiple mutations during replication [19,20]. In this context, it is crucial to study the host factors and compounds that can enhance or reduce replication of SARS-CoV-2 [21–25].

We previously reported that XPO1 inhibitors, including leptomycin B (LMB) and Selinexor, enhanced the replication of oncolytic myxoma virus (MYXV), a member of the leporipoxvirus genus of *poxviridae*, in diverse types of cultured human cancer cells where intrinsic cellular pathways restrict virus replication [26]. Selinexor treatment reduced the formation of cytoplasmic DHX9 antiviral granules, which are involved in lowering MYXV late protein synthesis and replication [26]. These findings led us to further investigate the role of Selinexor-mediated inhibition of the XPO1 nuclear export pathway on other viruses such as coronavirus.

Here, we show that Selinexor treatment can enhance coronavirus replication in a cell-type-specific manner. Mouse hepatitis virus (MHV) replication was enhanced in both murine and human cell lines. Furthermore, the targeted knockdown of XPO1 using siRNA also enhanced coronavirus replication, suggesting the pro-coronavirus drug action is indeed related to the expected nuclear export pathway target. However, SARS-CoV-2 replication remained unaffected in most of the cell lines that were tested. These observations indicate that unlike other viruses, inhibition of the nuclear export pathway can have different effects on coronavirus replication in different cell types in vitro.

2. Materials and Methods

2.1. Biosafety

SARS-CoV-2-GFP virus infections and virus manipulations were conducted at biosafety level 3 (BSL-3) and rSARS-CoV-2 Δ3a/Δ7b virus experiments were conducted at BSL-2+ level in the Biodesign Institute at ASU using appropriate and IBC-approved personal protective equipment and protocols.

2.2. Cell Lines

The L2 murine fibroblast cell line, African green monkey kidney Vero E6 cells, Baby hamster kidney cells (obtained from American Type Culture Collection (ATCC), Manassas, VA, USA), and murine 17Cl1 cells were cultured and maintained using Dulbecco's modified Eagle's medium (DMEM) supplemented with 10% FBS, 100 U/mL of penicillin, and 100 μg/mL streptomycin. Calu-3 cells (ATCC: HTB-55) were cultured and maintained using

Eagle's Minimum Essential Medium (EMEM) supplemented with 10% FBS, 100 U/mL of penicillin, and 100 µg/mL streptomycin. The HeLa-MHVR cell line (human HeLa cell line expressing mouse coronavirus receptor mCEACAM1) was provided by Tom Gallagher at Loyola University and maintained using DMEM with 10% FBS, HEPES buffer, 100 U/mL of penicillin, 100 µg/mL streptomycin, MEM non-essential amino acids, and sodium pyruvate. Human A549 cells (A549^{A2T2}) expressing ACE2 and TMPRSS2 (ACE2plusC3-A549/ACE2/TMPRSS2) were purchased from ATCC (CRL-3560) and maintained with DMEM supplemented with 10% FBS, 100 U/mL of penicillin, and 100 µg/mL streptomycin. A549-MHVR (human A549 cell line expressing mouse coronavirus receptor mCEACAM1) and A549^{ACE2} (human A549 cell line expressing ACE2 receptor) were provided by Susan Weiss at the Perelman School of Medicine at the University of Pennsylvania and maintained with RPMI1640 media supplemented with 10% FBS, 100 U/mL of penicillin, and 100 µg/mL streptomycin [27].

2.3. Reagents and Antibodies

Rabbit polyclonal antibodies for XPO1 and the mouse monoclonal antibody against β-actin were purchased from Thermo Fisher Scientific, Waltham, MA, USA. HRP-conjugated goat anti-rabbit and anti-mouse IgG antibodies were purchased from Jackson Immuno Research Laboratories, West Grove, PA, USA. Selinexor (KPT330) was purchased from Apex Bio (Tokyo, Japan). Leptomycin B, Ratjadone A, and Anguinomycin A were purchased from Santa Cruz Biotechnology, Dallas, TX, USA.

2.4. Viruses

Mouse hepatitis coronavirus MHV A59 that expresses GFP was used for all the assays. rA59/S$_{MHV-2}$-EGFP is a recombinant MHV A59 virus that expresses the spike of MHV-2 in place of the WT protein and GFP [28–30]. MHVE-GFP was constructed using an MHV A59 reverse genetics system, essentially as previously described [31–34]. The coding sequence for the MHV envelope (E) protein was fused to the GFP gene with an intervening tetra glycine linker. The construct was cloned into ORF 4a/b in the G subclone of the MHV infectious clone using Sbfl and EcoRV restriction sites. The construct was designed to maintain the transcription regulatory sequences for both ORF 4 and ORF5. The virus was recovered after assembling the full-length genomic cDNA and transcription of full-length genomic RNA as previously described [31–34]. Following electroporation into baby hamster kidney cells, the virus was recovered and grown in murine 17CI1 cells, and passage 1 stock was grown in mouse 17Cl1 cells and titered in L2 cells by a plaque assay. The SARS-CoV-2-GFP virus was provided by Ralph Baric at the University of North Carolina Chapel Hill [35].

2.5. Viral Replication Assay

Viral titers in different cell lines were determined using a viral replication assay. The cells were seeded in 24-well plate (2×10^5 cells/well). The next day, the cells were treated for 1 h with different concentrations of nuclear export inhibitors diluted in the appropriate media used for growth of the specific cell lines. Virus was added to the cells (volume calculated based on different multiplicities of infection and incubated for 1 h at 37 °C in the presence of the inhibitors. After 1 h, the unbound virus was removed, the cells were washed with DPBS (Dulbecco's phosphate-buffered saline), and media with inhibitors were added for further incubation. Both the cells and media were collected at different time points and stored at −80 °C freezer until processing. Afterwards, different dilutions were prepared in the appropriate media and plated on cell lines and fluorescent foci were counted after 24 h using a fluorescent microscope. All assays and dilutions were performed in triplicate. For SARS-CoV-2, all infections and virus manipulations were conducted at

biosafety level 3 (BSL-3) in the Biodesign Institute using appropriate and IBC-approved personal protective equipment and protocols. For the plaque assay, samples were serially diluted 10-fold and absorbed on Vero cells at 37 °C for 1 h. The cells were overlaid with media plus 0.7% agarose and incubated for two days at 37 °C. The cells were fixed with 4% paraformaldehyde and subsequently stained with 1% crystal violet to count the plaques.

2.6. siRNA Transfection and Western Blot Analysis

ON-TARGETplus SMART pool siRNAs for exportin 1/XPO1 and a non-targeting control (NT siRNA) were purchased from Dharmacon (Horizon Discovery, Lafayette, CO, USA). In 24-well plates, the cells were seeded with 40–50% confluence, left overnight for adherence, and then transfected with siRNAs (40 nM) using a Lipofectamine RNAiMAX (Invitrogen, Waltham, MA, USA) transfection reagent. After 48 h of transfection, the cells were infected with different MOIs of the virus for 1 h, washed to remove the unbound virus, and incubated with complete media. At the indicated time points, the cells were either observed by fluorescence microscopy to monitor and record the expression of fluorescent proteins or harvested and processed for titration of the progeny virions. For the detection of proteins, a Western blot analysis was performed from the total proteins as described before [36]. The blot image was acquired through the Amersham ImageQuant 800 imaging system (Cytiva, Marlborough, MA, USA). Semi-quantification of the bands was carried out using the ImageJ digital imaging processing software version 1.54 (https://imagej.net (accessed on 16 February 2025)).

2.7. Cell Viability Assay

To assess the viability of different cell lines after Selinexor treatment, 10,000 cells were seeded into each well of a 96-well plate. The next day, the cells were treated with different concentrations of Selinexor. A minimum of four to five wells were used for each treatment condition, and untreated cells (mock) served as controls. Cell viability at different time points was assessed using MTS reagents (Promega, Madison, WI, USA) according to the manufacturer's instructions.

2.8. Statistical Analysis

Statistical analyses were performed using GraphPad Prism software version 10. Values are represented as mean $\pm$ SD for at least two or three independent experiments. ANOVA and *t*-test (when only two groups were compared) were used to determine the significance. *p* values are reported as follows: not significant (ns), $p > 0.05$, * $p < 0.05$, ** $p < 0.01$, *** $p < 0.001$, and **** $p < 0.0001$.

3. Results

3.1. Nuclear Export Inhibitors Enhance Gene Expression and Replication of Mouse Hepatitis Virus in Murine L2 Cells

Murine L2 cells are naturally infected by the mouse hepatitis virus (MHV). We first tested whether inhibition of the XPO1-mediated nuclear export pathway in L2 cells by different SINEs can alter the replication of MHV. Since these compounds including Leptomycin B (LMB) are toxic to the cells above a 1 µM concentration, we used lower concentrations that had minimal or no cytotoxicity to the cells after 24 h. To our surprise, all the tested SINEs, including LMB, significantly enhanced MHV replication with a concentration of 0.1 µM and 0.01 µM (Figure 1A–C). Compared to untreated cells, treatment with the XPO1 inhibitor Ratjadone enhanced the virus titer by almost 1.0 log, whereas Anguinomycin and LMB enhanced the virus titer by about 0.7 log. Based on these results, next, we tested the FDA-approved anticancer nuclear export inhibitor Selinexor in our subsequent experiments.
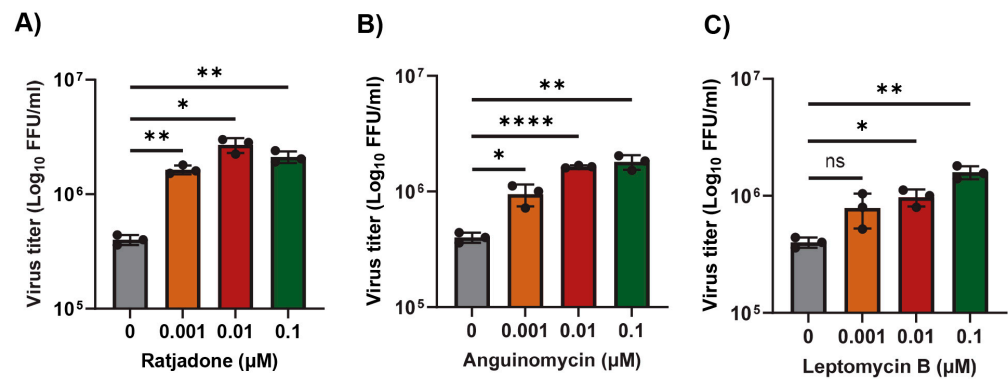
Figure 1. Nuclear export inhibitors enhance the replication of MHV in L2 cells. L2 cells were plated in 24-well plates and treated with the indicated concentration of nuclear export inhibitors (**A**) Ratjadone, (**B**) Anguinomycin, and (**C**) Leptomycin B for 1h and infected with the MHVE-GFP virus with an MOI of 0.01. Virus replication was measured by a plaque assay from the total number of viruses in the cells and supernatant 24 h post infection. Data represent $\pm$ SD and n = 3. Statistically significant differences in comparison to 24 hpi infection are indicated. ^{ns} $p > 0.05$, * $p < 0.05$, ** $p < 0.01$, **** $p < 0.0001$.

We monitored and measured the viability of L2 cells in response to treatment with different concentrations of Selinexor (Figure 2A). L2 cell viability was reduced only after treatment with a Selinexor concentration of 5 μM or above but had minimal or no effect with a concentration of 1 μM or less. To test the effect of Selinexor on MHV replication, L2 cells were first pretreated with different concentrations of Selinexor for one hour and infected with a GFP-expressing MHV A59 (rA59/S_{MHV-2}-EGFP) to monitor the level of GFP expression in the infected cells [28–30]. Infection with this MHV exhibits reduced cell fusion since the virus expresses a less fusogenic form of the spike protein and thus allowed for counting the number of GFP-positive cells. We observed an increased % of GFP expressing cells when they were pretreated with Selinexor (Figure 2B). At 16 hpi, compared to untreated cells, we observed a significantly increased % of GFP-positive cells after treatment with more than 1 μM Selinexor. However, after 24 hpi, even the 0.0001 μM Selinexor treatment showed a significantly increased % of GFP-expressing cells (Figure 2C). To assess the number of viruses produced in the presence of Selinexor, L2 cells were treated with different concentration of Selinexor and infected with another GFP expressing MHV A59 (MHVE-GFP) that expresses a highly fusogenic form of spike and readily forms plaques. After 24 h post infection, the infected cells and supernatant were collected to titer the progeny virus formation by a plaque assay. The virus titration results show a significantly enhanced number of viruses in the cells pretreated with Selinexor between the 1 and 10 μM concentrations (Figure 2D). These results confirm that Selinexor enhances MHV replication and progeny virus formation in naturally permissive L2 cells.
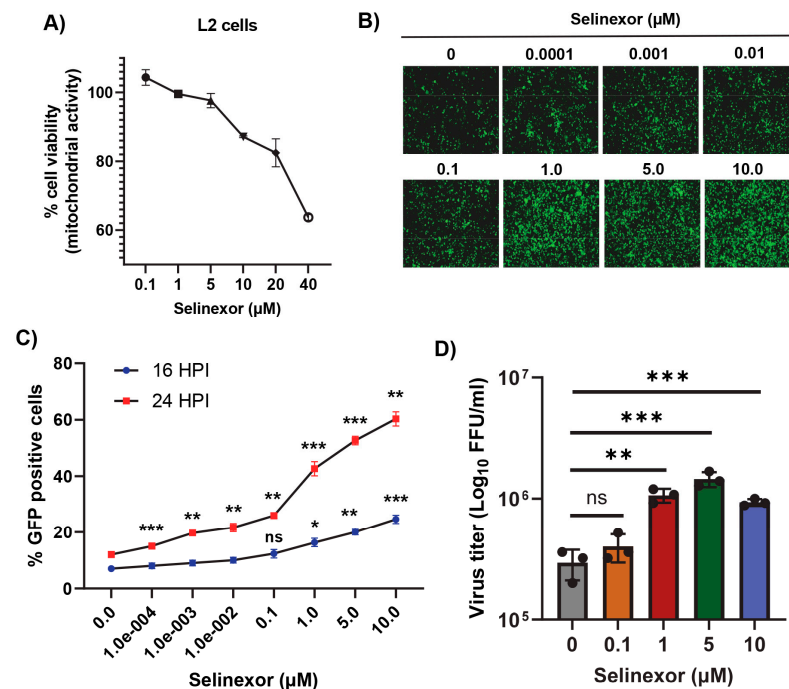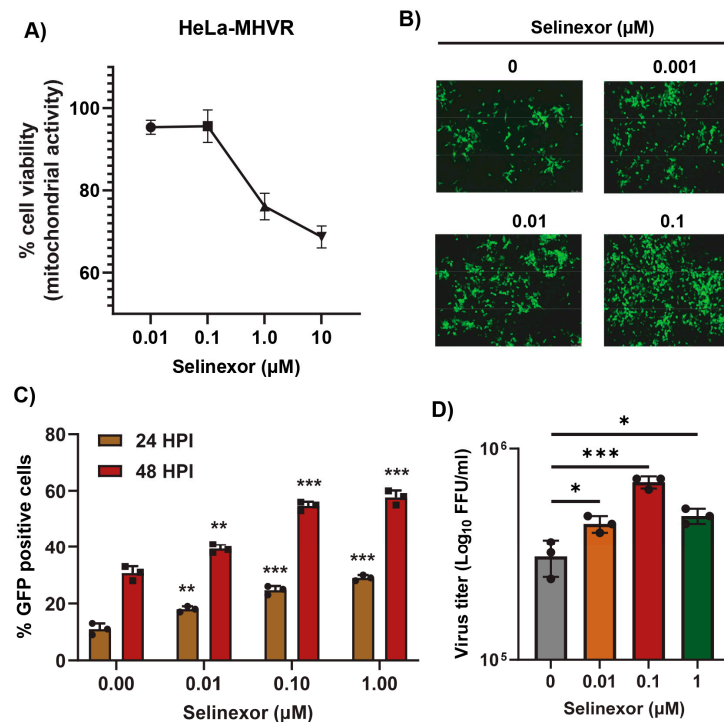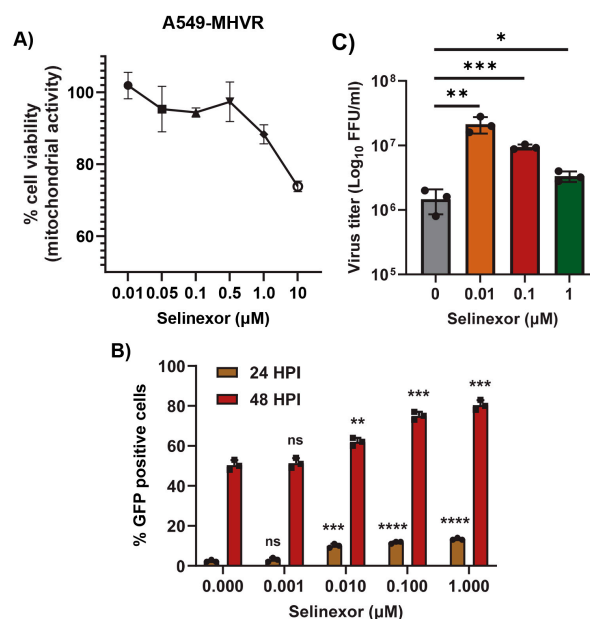
Figure 2. Selinexor enhances the replication of MHV in L2 cells. (**A**) Effect of Selinexor on L2 cells viability. Cells were plated in 96-well plates and treated with different concentrations of Selinexor, and cell viability was measured after 48 h. (**B–D**) Effect of Selinexor on MHV virus gene expression and replication. Cells were plated in 24-well plates, treated with the indicated concentration of Selinexor for 1 h, and infected with rA59/S_{MHV-2}-EGFP or MHVE-GFP virus with an MOI of 0.01. (**B**) Fluorescence images were taken 24 h post infection with rA59/S_{MHV-2}-EGFP; (**C**) percent of GFP-positive cells was counted using the Countess II cell counter at different time points after infection with rA59/S_{MHV-2}-EGFP; (**D**) MHVE-GFP virus replication was measured by a plaque assay from the total number of viruses in the cells and supernatant 24 h post infection. Data represent ± SD and $n = 3$. Statistically significant differences in comparison to the control are indicated. ^{ns} $p > 0.05$, * $p < 0.05$, ** $p < 0.01$, *** $p < 0.001$.

3.2. Selinexor Enhances Gene Expression and Replication of Mouse Hepatitis Virus in Human Cells

To further confirm that the effects of Selinexor on MHV replication are not cell-specific, we used human cell lines expressing MHV receptor (MHVR) carcinoembryonic antigen-related cell adhesion molecule 1 (CEACAM1), HeLa-MHVR (human HeLa cell line expressing MHVR) [37], and A549-CEACAM1/MHVR (human A549 cell line expressing MHVR) [27]. Both cell lines were first treated with different concentrations of Selinexor to test cell viability (Figures 3A and 4A). Unlike L2 cells, Selinexor concentrations above 1 μM significantly reduced the viability of the human cells. However, with a concentration of less than 0.1 μM, we observed minimal or no reduction in cell viability. To assess whether Selinexor enhances MHV replication in the human cell lines, both were pretreated with different concentrations of Selinexor for one hour and infected with a GFP-expressing MHV, rA59/S_{MHV-2}-EGFP, to monitor GFP expression in the infected cells. We observed enhanced GFP expressions when they were pretreated with Selinexor at a concentration of 0.01 μM or more (Figure 3B). Enhanced GFP expression was further confirmed by counting the number of GFP-positive cells (Figures 3C and 4B). To assess the amount of virus produced in the presence of Selinexor, HeLa-MHVR (Figure 3D) and A549-MHVR (Figure 4C) cells were treated with different concentrations of the drug and infected with MHVE-GFP. Again, like L2 cells, we observed significantly enhanced virus production in both the human cell lines when they were pretreated with Selinexor between the 1 and 0.01 μM concentrations (Figures 3D and 4C).

Figure 3. Selinexor enhances the replication of MHV in human HeLa-MHVR cells. (**A**) Effect of Selinexor on the viability of HeLa-MHVR cells. Cells were plated in 96-well plates and treated with different concentrations of Selinexor, and cell viability was measured after 48 h. (**B**–**D**) Effect of Selinexor on MHV virus replication in HeLa-MHVR cells. Cells were plated in 24-well plates, treated with the indicated concentration of Selinexor for 1h, and infected with $rA59/S_{MHV-2}$-EGFP or MHVE-GFP virus with an MOI of 0.01. (**B**) Fluorescence images were taken 24 h post infection with $rA59/S_{MHV-2}$-EGFP; (**C**) percent of GFP-positive cells at 24 h and 48 h post infection with $rA59/S_{MHV-2}$-EGFP was counted using the Countess II cell counter; (**D**) total number of viruses in the cells and supernatant was determined by a plaque assay 24 h post infection of cells with MHVE-GFP. Data represent $\pm$ SD and n = 3. Statistically significant differences in comparison to the control are indicated. * $p < 0.05$, ** $p < 0.01$, *** $p < 0.001$.
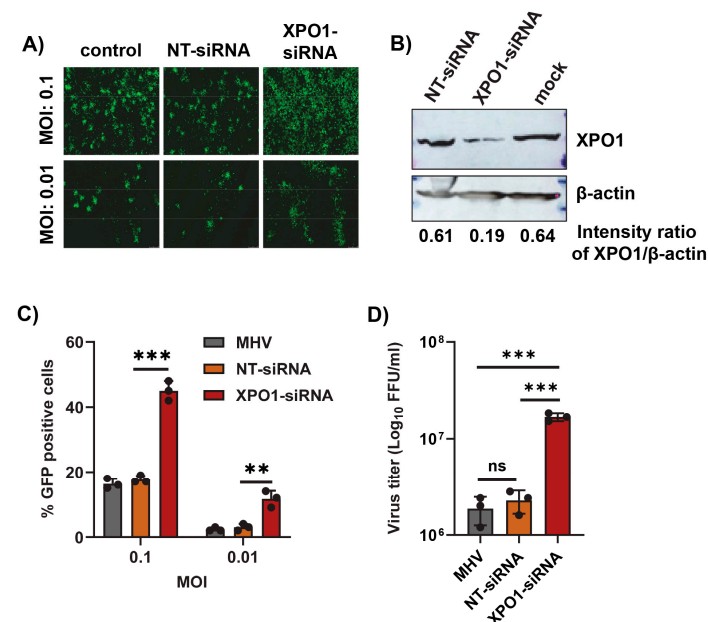

Figure 4. Selinexor enhances the replication of MHV in human A549-MHVR cells. (**A**) Effect of Selinexor on the viability of A549-MHVR cells. Cells were plated in 96-well plates and treated with

different concentration of Selinexor, and cell viability was measured after 48 h. (**B**,**C**) Effect of Selinexor on MHV virus replication in A549-MHVR cells. Cells were plated in 24-well plates, treated with the indicated concentration of Selinexor for 1h and infected with rA59/S_{MHV-2}-EGFP or MHVE-GFP virus with an MOI of 0.01. (**B**) Percent of GFP-positive cells at 24 h and 48 h post infection with rA59/S_{MHV-2}-EGFP was counted using the Countess II cell counter. (**C**) Total number of viruses in the cells and supernatant was determined by a plaque assay 24 h post infection of cells with MHVE-GFP. Data represent $\pm$ SD and $n = 3$. Statistically significant differences in comparison to the control are indicated. [ns] $p > 0.05$, * $p < 0.05$, ** $p < 0.01$, *** $p < 0.001$, **** $p < 0.0001$.

3.3. XPO1 Knockdown Enhances Mouse Hepatitis Virus Replication

Since inhibition of the XPO1-mediated nuclear export pathway using Selinexor enhanced coronavirus replication, we further extended this observation by inducing the direct knockdown of XPO1 using siRNA. After the transfection of XPO1 siRNA or a non-targeting control siRNA (NT-siRNA) in A549-MHVR cells, the cells were infected with different MOIs of the GFP-expressing MHV, rA59/S_{MHV-2}-EGFP, or MHVE-GFP. An increase in GFP-expressing cells was observed only in the XPO1 knockdown cells (Figure 5A). Furthermore, the enhanced number of GFP-positive cells in the XPO1 knockdown cells compared to controls was confirmed by counting the number of GFP-positive cells (Figure 5C). The level of XPO1 protein knockdown using siRNA was confirmed by a Western blot analysis (Figure 5B). To quantify the number of progeny virions in the infected cells and supernatant, the cells were infected with MHVE-GFP and samples were collected 24 h post infection. Virus titration shows that virus production significantly increased in the XPO1 knockdown cells compared to the NT-siRNA control or cells infected with the virus alone (Figure 5D).


Figure 5. XPO1 knockdown enhances the replication of MHV in human A549-MHVR cells. Cells were plated in 24-well plates, transfected with control non-targeting siRNA (NT-siRNA) or XPO1 siRNA for 48 h, and infected with rA59/S_{MHV-2}-EGFP or MHVE-GFP for another 24 h. (**A**) Images were taken using a fluorescence microscope 24 h post infection with MHVE-GFP. (**B**) Knockdown of XPO1 was confirmed with a Western blot analysis using the anti-XPO1 antibody. Actin was used as the total protein loading control. (**C**) Percent of GFP-positive cells after infection with rA59/S_{MHV-2}-EGFP was counted using the Countess II cell counter. (**D**) Total number of viruses in the cells and supernatant was determined by a plaque assay 24 h post infection of cells with MHVE-GFP. Data represent $\pm$ SD and $n = 3$ or 4. Statistically significant differences in comparison to the control are indicated. [ns] $p > 0.05$, ** $p < 0.01$, *** $p < 0.001$.
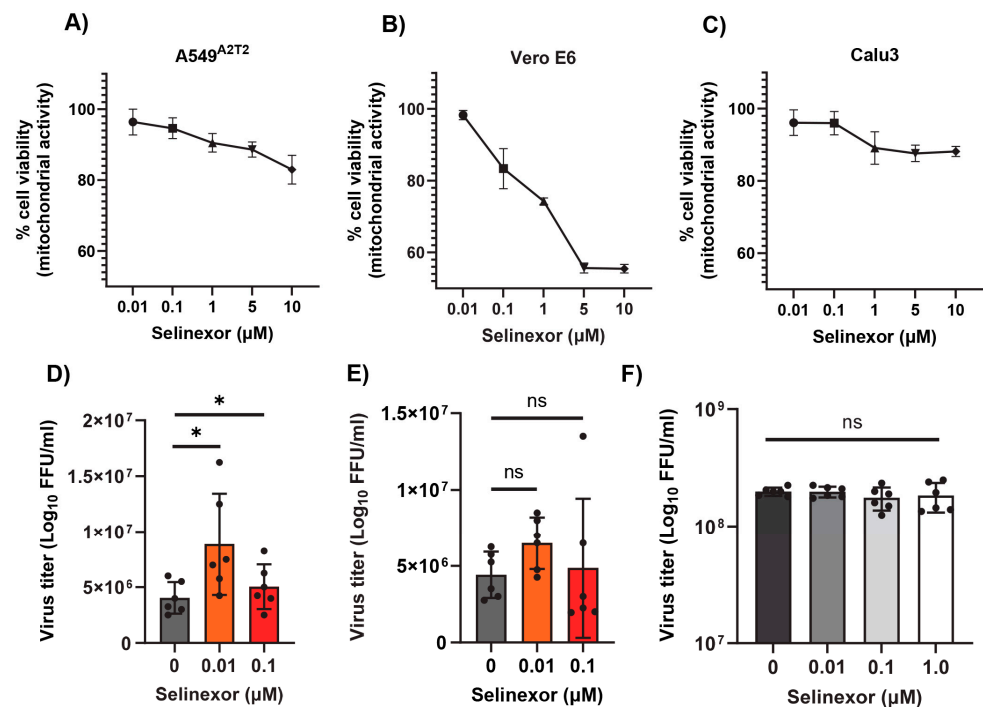
3.4. Effect of Selinexor on SARS-CoV-2 Replication

Next, we tested whether Selinexor enhances the replication of SARS-CoV-2 in human cells. We used a human A549 cell line expressing the ACE2 receptor (A549^{ACE2}) and a SARS-CoV-2 virus-expressing GFP (SARS-CoV-2-GFP) [35]. The A549^{ACE2} cell line showed a similar level of sensitivity to different concentrations of Selinexor like A549-MHVR (Figure 6A). To assess whether Selinexor enhances SARS-CoV-2 gene expression and replication, A549^{ACE2} cells were first pretreated with 0.01 µM of Selinexor for one hour and infected with SARS-CoV-2-GFP. After 24 h, the cells were collected and fixed to count the number of GFP-positive cells. A significantly increased number of GFP-positive cells was observed in the treated infected cells compared to the untreated cells (Figure 6B). We also observed a modest but significant increase in virus titer in the A549^{ACE2} cells (Figure 6C). The effect of Selinexor on SARS-CoV-2 was further tested using an infectious recombinant SARS-CoV-2 (rSARS-CoV-2) virus [38–40] in different cell lines. Human A549^{A2T2}, Vero E6, and human Calu3 cell lines were first treated with different concentrations of Selinexor to test cell viability (Figure 7A–C). All of these cell lines showed different levels of sensitivity to Selinexor. Like the parental SARS-CoV-2, the recombinant rSARS-CoV-2 virus titer was also increased in human A549^{A2T2} cells in the presence of Selinexor (Figure 7A). However, in Vero E6 and human Calu3 cells, no significant increase or decrease in virus titer was observed when treated with Selinexor (Figure 7B,C). These results indicate that, unlike MHV, the effect of Selinexor on the replication of SARS-CoV-2 is cell-type-dependent.
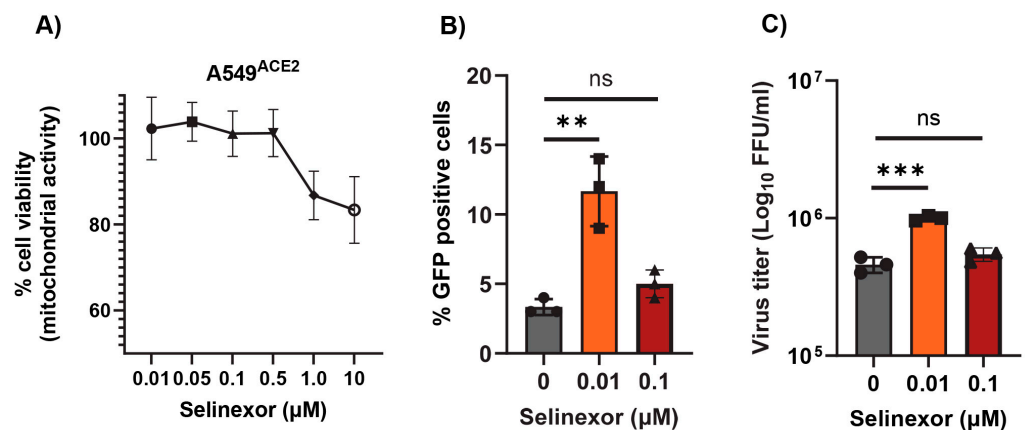
Figure 6. Effect of Selinexor on the replication of SARS-CoV-2 in human A549^{ACE2} cells. (**A**) Effect of Selinexor on the viability of A549^{ACE2} cells. Cells were treated with different concentration of Selinexor, and cell viability was measured after 48 h. Data represent mean ± SD, *n* = 4, and were normalized to the controls (mock). (**B**,**C**) Cells were plated in 12-well plates, treated with indicated concentration of Selinexor for 1h, and infected with the SARS-CoV-2 virus. (**B**) Percent of GFP-positive cells was counted using the Countess II cell counter after fixation of the cells. (**C**) Total number of progeny virus formation was measured by a plaque assay using Vero E6 cells. Data represent ± SD and *n* = 3 or 4. Statistically significant differences in comparison to the control are indicated. ^{ns} *p* > 0.05, ** *p* < 0.01, *** *p* < 0.001.

Figure 7. Effect of Selinexor on the replication of rSARS-CoV-2 in different cell types. (**A**) Human A549^{A2T2} cells, (**B**) Vero E6 cells, and (**C**) human Calu3 cells were plated in 96-well plates and treated with different concentration of Selinexor, and cell viability was measured after 48 h. Data represent mean $\pm$ SD, $n = 4$ or 5 and were normalized to the controls (mock). (**D**) Human A549^{A2T2} cells, (**E**) Vero E6 cells, and (**F**) human Calu3 cells were plated in 12-well plates, treated with the indicated concentration of Selinexor for 1h, and infected with the rSARS-CoV-2 virus with an MOI of 0.1. Total number of progeny virus formation was measured by a plaque assay using Vero E6 cells. Data represent $\pm$ SD and $n = 5$ or 6. Statistically significant differences in comparison to the control are indicated. ^{ns} $p > 0.05$, * $p < 0.05$.

4. Discussion

The nucleocytoplasmic transport process mediated by XPO1 plays a vital role in the export of hundreds of proteins from the nucleus. The proteins are involved in diverse cellular processes such as cell proliferation, cell cycle progression, and apoptosis [1,5]. Thus, the XPO1-mediated export pathway is targeted by viruses at various stages of their lifecycle to regulate cellular proteins and the appropriate localization of viral proteins [6,41]. Apart from viruses, this nuclear export pathway is also crucial for anticancer therapy due to the export of tumor suppressor proteins by XPO1 to the cytoplasm [7,10]. Therefore, XPO1 inhibitors are developed as potential antiviral and anticancer agents. The cysteine residue within the hydrophobic nuclear export sequence (NES)-binding region at position 528 is the prime target for most XPO1 inhibitors, including leptomycin B (LMB). LMB isolated from Streptomyces was the first specific inhibitor of XPO1 [42]. However, the clinical development was discontinued due to severe cell toxicity [43]. The irreversible binding of LMB with CRM1 caused long-term inhibition of CRM1-mediated nuclear export and possibly other off-target activities, resulting in cellular toxicity [43]. Synthetic derivatives of LMB with less toxicity due to the reversible binding with CRM1 have been clinically tested in humans. The FDA has approved one such XPO1/CRM1 inhibitor called Selinexor for treating hematological cancers [11]. XPO1 inhibitors have shown antiviral activity against many viruses, such as influenza; RSV; and recently, SARS-CoV-2 [13,25,41,44,45].

We reported that, unlike RNA viruses, LMB or Selinexor enhances the replication of oncolytic MYXV, a leporipoxvirus developed for cancer treatment [26]. In human cancer cells, Selinexor enhanced MYXV replication only at a low concentration that had minimal

or no toxicity to the cells. However, a higher concentration of Selinexor that caused cellular toxicity also reduced virus replication. Based on our observation that nuclear export inhibitors, including Selinexor, can enhance cytoplasmic replication of a poxvirus and a study showing that Selinexor inhibits SARS-CoV-2 replication, we first tested the effect of different nuclear export inhibitors, including Selinexor, on the replication of a mouse coronavirus MHV using murine L2 cells. To our surprise, we observed that pretreatment of L2 cells with different concentrations of these inhibitors that had minimal or no toxicity to the cells significantly increased the replication of MHV. This observation was further confirmed using human HeLa and A549 cells expressing the MHV receptor murine CEA-CAM1 [37]. Again, increased reporter GFP expression and MHV replication were observed when cells were pretreated with Selinexor concentrations that had minimal or no effect on the cell viability. These results confirm that the impact of Selinexor on MHV replication is independent of the cell type. Since XPO1 is the only known cellular target of Selinexor, we previously reported that XPO1 knockdown using siRNA enhanced the replication of MYXV in human cancer cells [26]. Here, again, we confirmed that XPO1/CRM1 knockdown also significantly enhanced the replication of MHV in both the A549-MHVR and HeLa-MHVR cell lines. Both poxviruses and coronaviruses replicate in the cytoplasm of infected cells. Observations that inhibition of the XPO1-mediated nuclear export pathway can enhance the replication of both viruses suggest the importance of this pathway for future studies to identify the host and viral proteins involved in this process. These results encouraged us to test whether the optimized lower concentration of Selinexor enhances SARS-CoV-2 replication in different cell types. However, unlike MHV, Selinexor-mediated enhanced SARS-CoV-2 replication was observed only in selected cell lines and had no significant effect on virus replication in other cell lines, such as Vero E6 and Calu3. This observation is in contrast to a previous study by Kashyap et al. showing that in Vero E6 cells, Selinexor treatment reduced the SARS-CoV-2 plaque number and virus titer by more than two logs with different concentrations of Selinexor [25]. In our study, we did not observe any reduction in virus titer with the tested concentration of Selinexor in any of the cell lines that we tested with both MHV and SARS-CoV-2. Further studies to understand the mechanism(s) of how inhibition of the cellular nuclear export pathway regulates coronavirus replication might help to resolve these observed differences. We observed the cell-type-specific effect of Selinexor on myxoma virus, where Selinexor did not affect virus replication in rabbit RK13 cells and Vero E6 cells [26]. Therefore, we can speculate that different cell types might respond to Selinexor differently against these tested viruses. For example, the XPO1 protein level is different in different cell types, and Selinexor is known to reduce the level of XPO1 proteins further [46–48]. Thus, the total amount of XPO1 proteins in different cell types after Selinexor treatment might impact the overall outcome of virus replication. However, the impact of XPO1 protein on coronavirus replication in different cell types has to be further explored. Inhibition of the XPO1-mediated nuclear export pathway results in several changes in the cells, such as cell cycle arrest and the modulation of cellular key signaling pathways regulating the expression of proinflammatory cytokines. Depending on the cell type, these cellular changes might impact the virus replication [49].

Selinexor is currently approved for treating selected hematological malignancies such as multiple myeloma and diffuse large B-cell lymphoma [11,50]. Multiple ongoing clinical trials are presently using Selinexor as a monotherapy or in combination with other treatments against diverse types of malignancies [51,52]. Our results indicate that Selinexor-mediated inhibition of the nuclear export pathway might have different effects on virus replication. Future studies should focus on how Selinexor and the nuclear transportation pathway regulate the replication of coronaviruses.

References

1. Wing, C.E.; Fung, H.Y.J.; Chook, Y.M. Karyopherin-mediated nucleocytoplasmic transport. *Nat. Rev. Mol. Cell Biol.* **2022**, *23*, 307–328. [CrossRef] [PubMed]
2. Tetenbaum-Novatt, J.; Rout, M.P. The mechanism of nucleocytoplasmic transport through the nuclear pore complex. *Cold Spring Harb. Symp. Quant. Biol.* **2010**, *75*, 567–584. [CrossRef] [PubMed]
3. Kumar, A.V.; Kang, T.; Thakurta, T.G.; Ng, C.; Rogers, A.N.; Larsen, M.R.; Lapierre, L.R. Exportin 1 modulates life span by regulating nucleolar dynamics via the autophagy protein LGG-1/GABARAP. *Sci. Adv.* **2022**, *8*, eabj1604. [CrossRef] [PubMed]
4. Ishikawa, C.; Mori, N. Exportin-1 is critical for cell proliferation and survival in adult T cell leukemia. *Investig. New Drugs* **2022**, *40*, 718–727. [CrossRef]
5. Azmi, A.S.; Uddin, M.H.; Mohammad, R.M. The nuclear export protein XPO1—from biology to targeted therapy. *Nat. Rev. Clin. Oncol.* **2021**, *18*, 152–169. [CrossRef]
6. Uddin, M.H.; Zonder, J.A.; Azmi, A.S. Exportin 1 inhibition as antiviral therapy. *Drug Discov. Today* **2020**, *25*, 1775–1781. [CrossRef]
7. Azizian, N.G.; Li, Y. XPO1-dependent nuclear export as a target for cancer therapy. *J. Hematol. Oncol.* **2020**, *13*, 61. [CrossRef]
8. Zhao, L.; Luo, B.; Wang, L.; Chen, W.; Jiang, M.; Zhang, N. Pan-cancer analysis reveals the roles of XPO1 in predicting prognosis and tumorigenesis. *Transl. Cancer Res.* **2021**, *10*, 4664–4679. [CrossRef]
9. Jans, D.A.; Martin, A.J.; Wagstaff, K.M. Inhibitors of nuclear transport. *Curr. Opin. Cell Biol.* **2019**, *58*, 50–60. [CrossRef]
10. Gerecitano, J. SINE (selective inhibitor of nuclear export)--translational science in a new class of anti-cancer agents. *J. Hematol. Oncol.* **2014**, *7*, 67. [CrossRef]
11. Goldsmith, S.R.; Liu, L.; Shiah, K. Selinexor therapy for multiple myeloma and non-Hodgkin lymphomas. *Curr. Opin. Oncol.* **2022**, *34*, 524–530. [CrossRef]
12. Lassman, A.B.; Wen, P.Y.; van den Bent, M.J.; Plotkin, S.R.; Walenkamp, A.M.E.; Green, A.L.; Li, K.; Walker, C.J.; Chang, H.; Tamir, S.; et al. A Phase II Study of the Efficacy and Safety of Oral Selinexor in Recurrent Glioblastoma. *Clin. Cancer Res. Off. J. Am. Assoc. Cancer Res.* **2022**, *28*, 452–460. [CrossRef] [PubMed]

13. Pickens, J.A.; Tripp, R.A. Verdinexor Targeting of CRM1 is a Promising Therapeutic Approach against RSV and Influenza Viruses. *Viruses* **2018**, *10*, 48. [CrossRef] [PubMed]

14. Sajidah, E.S.; Lim, K.; Wong, R.W. How SARS-CoV-2 and Other Viruses Build an Invasion Route to Hijack the Host Nucleocytoplasmic Trafficking System. *Cells* **2021**, *10*, 1424. [CrossRef] [PubMed]

15. Paules, C.I.; Marston, H.D.; Fauci, A.S. Coronavirus Infections-More Than Just the Common Cold. *JAMA* **2020**, *323*, 707–708. [CrossRef] [PubMed]

16. V'Kovski, P.; Kratzel, A.; Steiner, S.; Stalder, H.; Thiel, V. Coronavirus biology and replication: Implications for SARS-CoV-2. *Nat. Rev. Microbiol.* **2021**, *19*, 155–170. [CrossRef]

17. Fung, T.S.; Liu, D.X. Human Coronavirus: Host-Pathogen Interaction. *Annu. Rev. Microbiol.* **2019**, *73*, 529–557. [CrossRef]

18. Zhang, T.; Wu, Q.; Zhang, Z. Probable Pangolin Origin of SARS-CoV-2 Associated with the COVID-19 Outbreak. *Curr. Biol.* **2020**, *30*, 1346–1351.e1342. [CrossRef]

19. Mahilkar, S.; Agrawal, S.; Chaudhary, S.; Parikh, S.; Sonkar, S.C.; Verma, D.K.; Chitalia, V.; Mehta, D.; Koner, B.C.; Vijay, N.; et al. SARS-CoV-2 variants: Impact on biological and clinical outcome. *Front. Med.* **2022**, *9*, 995960. [CrossRef]

20. Wiegand, T.; Nemudryi, A.; Nemudraia, A.; McVey, A.; Little, A.; Taylor, D.N.; Walk, S.T.; Wiedenheft, B. The Rise and Fall of SARS-CoV-2 Variants and Ongoing Diversification of Omicron. *Viruses* **2022**, *14*, 2009. [CrossRef]

21. Madden, E.A.; Diamond, M.S. Host cell-intrinsic innate immune recognition of SARS-CoV-2. *Curr. Opin. Virol.* **2022**, *52*, 30–38. [CrossRef] [PubMed]

22. Lv, L.; Zhang, L. Host proviral and antiviral factors for SARS-CoV-2. *Virus Genes* **2021**, *57*, 475–488. [CrossRef] [PubMed]

23. Baggen, J.; Vanstreels, E.; Jansen, S.; Daelemans, D. Cellular host factors for SARS-CoV-2 infection. *Nat. Microbiol.* **2021**, *6*, 1219–1232. [CrossRef]

24. Narayanan, A.; Narwal, M.; Majowicz, S.A.; Varricchio, C.; Toner, S.A.; Ballatore, C.; Brancale, A.; Murakami, K.S.; Jose, J. Identification of SARS-CoV-2 inhibitors targeting Mpro and PLpro using in-cell-protease assay. *Commun. Biol.* **2022**, *5*, 169. [CrossRef]

25. Kashyap, T.; Murray, J.; Walker, C.J.; Chang, H.; Tamir, S.; Hou, B.; Shacham, S.; Kauffman, M.G.; Tripp, R.A.; Landesman, Y. Selinexor, a novel selective inhibitor of nuclear export, reduces SARS-CoV-2 infection and protects the respiratory system in vivo. *Antivir. Res.* **2021**, *192*, 105115. [CrossRef]

26. Rahman, M.M.; van Oosterom, F.; Enow, J.A.; Hossain, M.; Gutierrez-Jensen, A.D.; Cashen, M.; Everts, A.; Lowe, K.; Kilbourne, J.; Daggett-Vondras, J.; et al. Nuclear Export Inhibitor Selinexor Enhances Oncolytic Myxoma Virus Therapy against Cancer. *Cancer Res. Commun.* **2023**, *3*, 952–968. [CrossRef]

27. Li, Y.; Renner, D.M.; Comar, C.E.; Whelan, J.N.; Reyes, H.M.; Cardenas-Diaz, F.L.; Truitt, R.; Tan, L.H.; Dong, B.; Alysandratos, K.D.; et al. SARS-CoV-2 induces double-stranded RNA-mediated innate immune responses in respiratory epithelial-derived cells and cardiomyocytes. *Proc. Natl. Acad. Sci. USA* **2021**, *118*, e2022643118. [CrossRef]

28. Das Sarma, J.; Fu, L.; Tsai, J.C.; Weiss, S.R.; Lavi, E. Demyelination determinants map to the spike glycoprotein gene of coronavirus mouse hepatitis virus. *J. Virol.* **2000**, *74*, 9206–9213. [CrossRef]

29. Das Sarma, J.; Iacono, K.; Gard, L.; Marek, R.; Kenyon, L.C.; Koval, M.; Weiss, S.R. Demyelinating and nondemyelinating strains of mouse hepatitis virus differ in their neural cell tropism. *J. Virol.* **2008**, *82*, 5519–5526. [CrossRef]

30. Qiu, Z.; Hingley, S.T.; Simmons, G.; Yu, C.; Das Sarma, J.; Bates, P.; Weiss, S.R. Endosomal proteolysis by cathepsins is necessary for murine coronavirus mouse hepatitis virus type 2 spike-mediated entry. *J. Virol.* **2006**, *80*, 5768–5776. [CrossRef]

31. Verma, S.; Lopez, L.A.; Bednar, V.; Hogue, B.G. Importance of the penultimate positive charge in mouse hepatitis coronavirus A59 membrane protein. *J. Virol.* **2007**, *81*, 5339–5348. [CrossRef] [PubMed]

32. Ye, Y.; Hogue, B.G. Role of the coronavirus E viroporin protein transmembrane domain in virus assembly. *J.Virol.* **2007**, *81*, 3597–3607. [CrossRef] [PubMed]

33. Lopez, L.A.; Riffle, A.J.; Pike, S.L.; Gardner, D.; Hogue, B.G. Importance of conserved cysteine residues in the coronavirus envelope protein. *J. Virol.* **2008**, *82*, 3000–3010. [CrossRef]

34. Arndt, A.L.; Larson, B.J.; Hogue, B.G. A conserved domain in the coronavirus membrane protein tail is important for virus assembly. *J. Virol.* **2010**, *84*, 11418–11428. [CrossRef]

35. Hou, Y.J.; Okuda, K.; Edwards, C.E.; Martinez, D.R.; Asakura, T.; Dinnon, K.H., 3rd; Kato, T.; Lee, R.E.; Yount, B.L.; Mascenik, T.M.; et al. SARS-CoV-2 Reverse Genetics Reveals a Variable Infection Gradient in the Respiratory Tract. *Cell* **2020**, *182*, 429–446.e414. [CrossRef]

36. Rahman, M.M.; Bagdassarian, E.; Ali, M.A.M.; McFadden, G. Identification of host DEAD-box RNA helicases that regulate cellular tropism of oncolytic Myxoma virus in human cancer cells. *Sci. Rep.* **2017**, *7*, 15710. [CrossRef]

37. Rao, P.V.; Gallagher, T.M. Intracellular complexes of viral spike and cellular receptor accumulate during cytopathic murine coronavirus infections. *J. Virol.* **1998**, *72*, 3278–3288. [CrossRef]

38. Ye, C.; Chiem, K.; Park, J.G.; Oladunni, F.; Platt, R.N., 2nd; Anderson, T.; Almazan, F.; de la Torre, J.C.; Martinez-Sobrido, L. Rescue of SARS-CoV-2 from a Single Bacterial Artificial Chromosome. *mBio* **2020**, *11*, 10–1128. [CrossRef]

39. Ye, C.; Park, J.G.; Chiem, K.; Dravid, P.; Allué-Guardia, A.; Garcia-Vilanova, A.; Pino Tamayo, P.; Shivanna, V.; Kapoor, A.; Walter, M.R.; et al. Immunization with Recombinant Accessory Protein-Deficient SARS-CoV-2 Protects against Lethal Challenge and Viral Transmission. *Microbiol. Spectr.* **2023**, *11*, e0065323. [CrossRef]

40. Silvas, J.A.; Vasquez, D.M.; Park, J.G.; Chiem, K.; Allué-Guardia, A.; Garcia-Vilanova, A.; Platt, R.N.; Miorin, L.; Kehrer, T.; Cupic, A.; et al. Contribution of SARS-CoV-2 Accessory Proteins to Viral Pathogenicity in K18 Human ACE2 Transgenic Mice. *J. Virol.* **2021**, *95*, e0040221. [CrossRef]

41. Mathew, C.; Ghildyal, R. CRM1 Inhibitors for Antiviral Therapy. *Front. Microbiol.* **2017**, *8*, 1171. [CrossRef] [PubMed]

42. Ferreira, B.I.; Cautain, B.; Grenho, I.; Link, W. Small Molecule Inhibitors of CRM1. *Front. Pharmacol.* **2020**, *11*, 625. [CrossRef] [PubMed]

43. Newlands, E.S.; Rustin, G.J.; Brampton, M.H. Phase I trial of elactocin. *Br. J. Cancer* **1996**, *74*, 648–649. [CrossRef] [PubMed]

44. Perwitasari, O.; Johnson, S.; Yan, X.; Howerth, E.; Shacham, S.; Landesman, Y.; Baloglu, E.; McCauley, D.; Tamir, S.; Tompkins, S.M.; et al. Verdinexor, a novel selective inhibitor of nuclear export, reduces influenza a virus replication in vitro and in vivo. *J. Virol.* **2014**, *88*, 10228–10243. [CrossRef]

45. Mathew, C.; Tamir, S.; Tripp, R.A.; Ghildyal, R. Reversible disruption of XPO1-mediated nuclear export inhibits respiratory syncytial virus (RSV) replication. *Sci. Rep.* **2021**, *11*, 19223. [CrossRef]

46. Sexton, R.; Mahdi, Z.; Chaudhury, R.; Beydoun, R.; Aboukameel, A.; Khan, H.Y.; Baloglu, E.; Senapedis, W.; Landesman, Y.; Tesfaye, A.; et al. Targeting Nuclear Exporter Protein XPO1/CRM1 in Gastric Cancer. *Int. J. Mol. Sci.* **2019**, *20*, 4826. [CrossRef]

47. Zheng, Y.; Gery, S.; Sun, H.; Shacham, S.; Kauffman, M.; Koeffler, H.P. KPT-330 inhibitor of XPO1-mediated nuclear export has anti-proliferative activity in hepatocellular carcinoma. *Cancer Chemother. Pharmacol.* **2014**, *74*, 487–495. [CrossRef]

48. Chakravarti, N.; Boles, A.; Burzinski, R.; Sindaco, P.; Isabelle, C.; McConnell, K.; Mishra, A.; Porcu, P. XPO1 blockade with KPT-330 promotes apoptosis in cutaneous T-cell lymphoma by activating the p53-p21 and p27 pathways. *Sci. Rep.* **2024**, *14*, 9305. [CrossRef]

49. Li, D.; Fang, H.; Zhang, R.; Xie, Q.; Yang, Y.; Chen, L. Beyond oncology: Selinexor's journey into anti-inflammatory treatment and long-term management. *Front. Immunol.* **2024**, *15*, 1398927. [CrossRef]

50. Nachmias, B.; Schimmer, A.D. Targeting nuclear import and export in hematological malignancies. *Leukemia* **2020**, *34*, 2875–2886. [CrossRef]

51. Landes, J.R.; Moore, S.A.; Bartley, B.R.; Doan, H.Q.; Rady, P.L.; Tyring, S.K. The efficacy of selinexor (KPT-330), an XPO1 inhibitor, on non-hematologic cancers: A comprehensive review. *J. Cancer Res. Clin. Oncol.* **2022**, *149*, 2139–2155. [CrossRef]

52. Galinski, B.; Alexander, T.B.; Mitchell, D.A.; Chatwin, H.V.; Awah, C.; Green, A.L.; Weiser, D.A. Therapeutic Targeting of Exportin-1 in Childhood Cancer. *Cancers* **2021**, *13*, 6161. [CrossRef]